**Libyan Med J.** 2025;17(3):366-377
https://doi.org/10.69667/lmj.2517402
**Libyan Medical Journal**
https://lmj.ly/index.php/ojs/index *eISSN: 2079-1224*

*Original article*

# Detection of Radioactive Element Contents and their Hazard indices in Composite Soil and Rock Samples from the Southern Al Jabal al Akhdar Region (Between Aslunta and Al Makhili), Libya

**Hamad Hasan*[1], Hanan Bader[1], Huda Ali[2], Hani Othman[3]**

[1]*Chemistry Department, Faculty of Science, Omar Al-Mukhtar University, Libya*
[2]*Chemical Engineering Department, Faculty of Engineering, Omar Al-Mukhtar University, Libya*
[3]*Natural resources, Faculty of Natural Resources and Environmental Sciences, Omar Al-Mukhtar University, Libya*
***Corresponding email***. *hamad.dr@omu.edu.ly*

***Keywords***:
*Radioactive Elements, Soil, Rock Samples, $^{226}Ra$, $^{238}U$, $^{232}Th$, $^{40}K$.*

***A B S T R A C T***

*The current study aims to reveal the contents of radioactive elements in soil and rock samples collected from the southern area of the Green Mountain, extending between Al-Salanta and Al-Makhili. Soil samples were taken from 20 areas, and the experimental design was a completely randomized block design with three replications. The most important results obtained are as follows: The results of this study showed the presence of several natural radioactive elements with various uses, which can be considered important natural resources. The presence of radioactive potassium (40K), uranium (238U), thorium (232Th), and radium (226Ra) were recorded, and these are natural radioactive elements that can be found in many soils. The results of this study recorded radioactive potassium concentrations ranging between (63.65– 403.56 Bq/kg), with the highest concentration found at site number 11, known as the (Al-Qarrah Al-Hamra area near the Tanmalo region), while the lowest concentration was at site 13, known as the (Tanmalo area). Regarding the results related to radioactive uranium 238, this study recorded concentrations ranging between (38.34–82.66 Bq/kg), with the highest concentrations found at site number (2), in the area of Wadi A'teer near the Aslanta area, while the lowest concentrations were at site number (9), in the area of Qlay'at near the Crushers area. Generally, the study results recorded highly significant changes at the level of 0.0001. The results related to radioactive radium showed that its concentrations ranged between (32.005–96.48 Bq/kg), with the highest concentrations found at site number (2), in the area of Wadi A'teer near the Aslinta area, while the lowest concentrations were at site number (9), in the area of Qlay'at near the quarries. Generally, the study results recorded highly significant changes at the level of 0.0001. Regarding the results related to radioactive thorium-232, this study recorded concentrations ranging between (31.15-63.18 Bq/kg), with the highest concentrations found at site number (6), in the area of (Mas'ada near Jirdas), while the lowest concentrations were at site number (20), in the area of (North Gate 1 near Al-Mukhayli). In general, the study results showed highly significant changes at the level of 0.0001. The study results recorded a clear variation in the concentrations of natural radioactive elements in the study areas. The results showed the presence of natural radioactive elements in all soils of the study sites. The following figures illustrate the distribution of radioactive elements in the study areas. When comparing the recorded results of the current study with others in different parts of the world, we find that the potassium concentration rate recorded an increase compared to the other radioactive elements in the study area, but was lower than the global average value. Additionally, the activity concentration rates of radium and thorium were lower than the global average value.*

## Introduction

The spatial distribution of radionuclides within terrestrial environments is inherently heterogeneous, contingent upon both the region's lithological characteristics and anthropogenic perturbations [1]. Environmental radioactivity primarily originates from naturally occurring primordial radionuclides, such as $^{40}K$ and the decay series of $^{232}Th$ and $^{238}U$, which are ubiquitously distributed in geological formations and constitute the principal component of the natural background radiation [2, 3]. These isotopes, present since the Earth's formation, are classified as primordial sources and reside in significant quantities within soil, which acts as a major reservoir for natural radioactivity [4, 5]. Additional contributions to the total radiation dose include cosmogenic sources and anthropogenic activities, including hydrocarbon exploration, agricultural practices, and nuclear testing, which can elevate ambient concentrations of radioactive materials [5]. Notably, regions subjected to mining operations are often inadequately characterized, potentially leading to an underestimation of localized radioisotope concentrations. This spatial variability necessitates the application of diverse measurement methodologies for accurate


***Received***: *02-08-2025* - ***Accepted***: *03-10-2025* - ***Published***: *11-10-2025*

**Libyan Med J.** 2025;17(3):366-377
https://doi.org/10.69667/lmj.2517402
**Libyan Medical Journal**
https://lmj.ly/index.php/ojs/index *eISSN: 2079-1224*

environmental monitoring [1]. While previous research in Libya has initiated the estimation of radioactive elements [6-8] alongside broader environmental studies on various pollutants [9-89], comprehensive assessments in specific geological settings remain limited. Therefore, the primary objective of this investigation is to determine the concentrations of radioactive elements in soil and rock samples collected from the southern vicinity of the Al-Gabal Al-Akhder region, Libya, and to calculate relevant radiological hazard indices.

## Methods

### *Study Area*

The study area, a semi-arid zone, is located in the southeastern part of the Al Jabal al Akhdar Governorate in northeastern Libya, approximately 27 km from Al Bayda. This climatic condition contrasts with the predominantly semi-humid climate of the wider Al Jabal al Akhdar (Cyrenaica) region, which receives an average annual precipitation of 380 mm. The investigation focused on a geographic corridor bounded by the coordinates 19°32'16.12" N to 34°32'50.40" N latitude and 17°22'45.81" E to 43°21'49.18" E longitude, extending for approximately 100 km between Aslunta and Al Makhili.

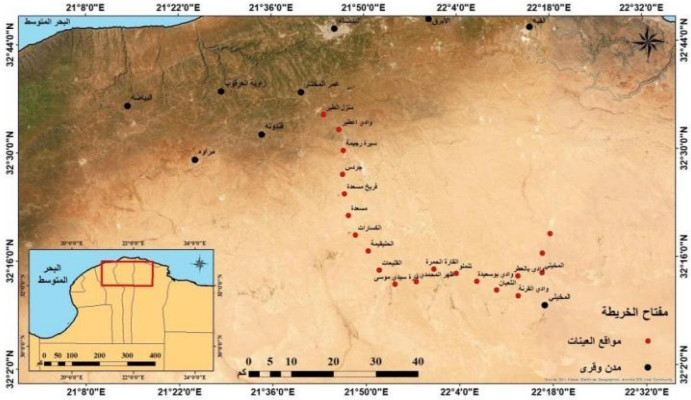


***Figure 1. Map of the study area locations***

***Table 1: The names and numbers of the sample collection areas***

| Simple No | Site Name |
|---|---|
| **P1** | Aslanta |
| **P2** | Wadi Atir |
| **P3** | Sira Rajima |
| **P4** | Jirdas |
| **P5** | Freikh Mas'ada |
| **P6** | Mas'ada |
| **P7** | Al-Kasarat |
| **P8** | Al-Halaqiema |
| **P9** | Al-Qulay'at |
| **P10** | Qara Sidi Musa |
| **P11** | Al-Qara Al-Hamra |
| **P12** | Zahr Al-Muhamadi |
| **P13** | Tanmilu |
| **P14** | Wadi Bousa'ida |
| **P15** | Al-Thuban |
| **P16** | Wadi Al-Qurna |
| **P17** | Wadi Bil'atar |
| **P18** | Al-Mukhayli |
| **P19** | 2 North of the Gate District |
| **P20** | 1 North of the Gate District |

### *Sample Collection and Preparation*

A total of twenty soil samples were collected from distinct locations within the study area at a uniform depth of 20 cm. Each sample was processed by pulverizing it into a fine powder and manually sieving through a 1 mm mesh to achieve particle homogeneity and remove extraneous materials. The


***Received****: 02-08-2025 -* ***Accepted****: 03-10-2025 -* ***Published****: 11-10-2025*

Libyan Med J. 2025;17(3):366-377
https://doi.org/10.69667/lmj.2517402
Libyan Medical Journal
https://lmj.ly/index.php/ojs/index eISSN: 2079-1224

homogenized samples were then oven-dried at a temperature of 105°C for a period of 24 hours to eliminate moisture. Subsequently, the dried samples were weighed and transferred to Marinelli beakers (cylindrical plastic containers). The beakers were hermetically sealed to prevent the escape of radon gas ($^{222}$Rn) and stored for four weeks to allow for the establishment of secular equilibrium between $^{226}$Ra and its short-lived decay progeny prior to radiometric analysis.

***Detection of Radioactive Elements***

The identification and quantification of natural radionuclides were performed using gamma-ray spectrometry. The measurement system consisted of a NaI(Tl) scintillation detector coupled with a high-voltage power supply and a computer equipped with software for spectral acquisition and analysis. System calibration was executed using certified gamma-ray standard sources. All measurements were conducted at the Physics Department, Faculty of Science, Omar Al-Mukhtar University [7-9].

***Estimation of Radium Emanation Rate in Geological Samples***

The radium emanation rate was determined using the "can technique" [90]. Initially, 250 g aliquots of the dried and pulverized soil samples were sealed in 1-liter glass containers for 45 days to ensure equilibrium between radium and its progeny. Following this, LR-115 Type II solid-state nuclear track detectors (SSNTDs) were affixed to the inner upper surface of the containers, which were then resealed for a 90-day exposure period to record alpha particles from radon decay. Post-exposure, the detectors were chemically etched in a 2.5 N NaOH solution maintained at 50°C for 3 hours in a constant-temperature water bath. The resulting track densities (tracks cm$^{-2}$) were measured using an Olympus optical microscope at 400X magnification, and radium concentrations were calculated accordingly.

***Estimation of Uranium in Soil Samples***

Uranium concentrations were quantified via the fission track technique [90]. Geological samples were pulverized and homogenized with a polyvinyl chloride (PVC) binder, and the mixture was hydraulically pressed into thin pellets. These pellets were encapsulated in aluminum foil and placed in close contact with Lexan plastic track detectors alongside certified reference standards (Fischer glass). The assembly was irradiated with a thermal neutron fluence of approximately $1 \times 10^{15}$ n cm$^{-2}$. Fission fragments from the $^{235}$U(n,f) reaction induced latent tracks in the Lexan detectors, which were subsequently revealed by chemical etching in a 6.25 N NaOH solution at 60°C for 50 minutes. The density of the fission tracks was determined using an optical microscope at 400X magnification, and uranium concentrations were calculated by comparing the track densities of the samples to those of the standards.

***Calculation of Radiation Hazard Indices***

To assess the potential radiological health risks associated with elevated concentrations of naturally occurring radionuclides, several internationally recognized hazard indices were computed from the measured activity concentrations of $^{238}$U, $^{232}$Th, and $^{40}$K.

***Radium Equivalent Activity (Raeq)***

The Radium Equivalent Activity (Raeq) was calculated to evaluate the gamma radiation hazard from the combined activity of $^{238}$U, $^{232}$Th, and $^{40}$K. This index provides a single weighted value that is commonly used to assess the suitability of construction materials. The Raeq was calculated using the established mathematical formula from previous studies [91].

**Raeq = AU + 1.43ATh + 0.07AK**

***Radionuclide Determination via Gamma Spectrometry***

Natural radionuclides were identified using sodium iodide (NaI) gamma-ray spectrometry. Specific radiation indices were calculated as follows: Radium Equivalent Activity (Raeq): The activity concentration (Bq/kg) for each radionuclide was determined using the equation:

**A = N / (εγ * Iγ * m * t) (1)**

Where: N = Net sample count (or net area under the photopeak), εγ = Detector efficiency, Iγ = Gamma yield, m = Sample mass, t = Counting time.

To evaluate radiation exposure, concentrations of $^{226}$Ra, $^{232}$Th, and $^{40}$K were analyzed, and a standard radiation hazard index was established. This index, known as the Radium Equivalent Activity (Raeq), is mathematically defined as [92].

**Raeq = ARa + 1.43ATh + 0.077AK (2)**

Where: ARa, ATh, AK = Activity concentrations of $^{226}$Ra, $^{232}$Th, and $^{40}$K, respectively.


**Received**: 02-08-2025 - **Accepted**: 03-10-2025 - **Published**: 11-10-2025

Libyan Med J. 2025;17(3):366-377
https://doi.org/10.69667/lmj.2517402
Libyan Medical Journal
https://lmj.ly/index.php/ojs/index eISSN: 2079-1224

***Radiation Hazard Indices (Hex and Hin)***

The detrimental effects of gamma radiation from radionuclides present in the soil samples were estimated by calculating various hazard indices. While total activity concentration serves as a precise indicator of overall radiation risk, these hazard indices also guide the selection of suitable materials for constructing dwellings, bricks, and other materials for human habitation. Two hazard indices were employed: the External Hazard Index (Hex) and the Internal Hazard Index (Hin). External Hazard Index (Hex): The external hazard index (Hex) due to gamma ray emission from the samples was calculated to estimate biological risk using the relationship:

**Hex = ARa/370 + ATh/259 + AK/4810 ≤ 1**

Where: ARa, ATh, and AK are the activity concentrations of $^{226}$Ra, $^{232}$Th, and $^{40}$K in Bq/kg

***Internal Hazard Index (Hin)***

Internal exposure arises from inhalation of radon gas ($^{222}$Rn) and its short-lived decay products or ingestion of other radionuclides. As radon is carcinogenic and present in all building materials, the measurement of radon exposure is termed the Internal Hazard Index, calculated as follows:

**Hin = ARa/185 + ATh/259 + AK/4810**

Gamma Level Index (Iγ): The gamma level index (Iγ) is used to assess the risk level from $^{238}$U, $^{232}$Th, and $^{40}$K radionuclides. It is calculated using the relationship:

**Iγ = ARa/150 + A Th/100 + AK/1500**

Where: ARa, ATh, and AK are the activity concentrations of $^{226}$Ra, $^{232}$Th, and $^{40}$K in Bq/kg [93].

***Alpha Index (Iα)***

External radiation, particularly radon and its short-lived decay products, poses a risk to the respiratory system. These emit alpha particles that adhere to airborne aerosols, dust, and other particles. Upon inhalation, radon decay products deposit on the cells lining the airways, where alpha particles can damage DNA and potentially cause lung cancer. The excess alpha radiation due to radon inhalation is estimated by the alpha index (Iα), defined as follows:

**Iα = ARa/200**

The recommended upper limit for $^{226}$Ra concentration is 200 Bq/kg, corresponding to Iα = 1.

***Computer Software***

Microsoft Excel and Origin software were utilized for data analysis and calculations in this study.

***Sample Preparation for NaI Detector***

In preparation for radiometric analysis, soil and vegetable samples were oven-dried at 95°C for a duration of 3-4 hours to ensure complete desiccation. The dried samples were then pulverized, homogenized, and sieved through a 200-mesh screen to obtain a fine, representative composite. Aliquots of these samples were subsequently weighed and sealed in 250 cm$^3$ polyethylene containers. To achieve secular equilibrium between the long-lived parent radionuclides ($^{238}$U and $^{232}$Th) and their short-lived decay progeny, the containers were hermetically sealed for a period of one month prior to measurement. This procedure is critical for preventing the escape of radon gas ($^{222}$Rn) and ensuring its decay products remain within the sample matrix. Each sealed sample was positioned directly atop the NaI(Tl) detector for a counting duration of 70,000 seconds, with results expressed in activity concentrations (Bq kg$^{-1}$). Quantification of the radionuclides was achieved by analyzing specific gamma-ray photopeaks. The activity of $^{226}$Ra was determined from its 186.2 keV peak. For the $^{238}$U decay series, activity was derived from the gamma lines of its progeny: $^{214}$Pb (295.2 keV and 351.9 keV) and $^{214}$Bi (609.3 keV, 768.4 keV, 1120.3 keV, 1238.1 keV, 1377.7 keV, and 1764.5 keV). Similarly, the $^{232}$Th series activity was quantified using photopeaks from $^{228}$Ac (92 keV, 209.5 keV, 338.5 keV, 911.1 keV, 968.9 keV), $^{208}$Tl (583 keV), and $^{212}$Bi (727.2 keV). The activity of $^{40}$K was determined from its prominent 1460 keV gamma line [94].

## Results

The distribution of natural radionuclides in terrestrial environments is fundamentally governed by local geological conditions. Natural radioactivity in soil is primarily quantified by the activity concentrations of the $^{238}$U series, $^{232}$Th series, and $^{40}$K. In radiological assessments, the $^{238}$U series is often represented by the activity of $^{226}$Ra, as its subsequent decay progeny contribute predominantly to the gamma radiation dose. The terrestrial component of natural background radiation, which contributes to the total radiation exposure of populations, is therefore directly dependent on the geochemical composition of underlying soils and rocks.


**Received**: 02-08-2025 - **Accepted**: 03-10-2025 - **Published**: 11-10-2025

Libyan Med J. 2025;17(3):366-377
https://doi.org/10.69667/lmj.2517402
Libyan Medical Journal
https://lmj.ly/index.php/ojs/index eISSN: 2079-1224

***Radioactive Potassium ($^{40}K$)***

The measured activity concentrations of $^{40}K$, detailed in Table 2, exhibited significant spatial variation across the 20 sampling sites. The maximum concentration of $^{40}K$ was observed at the Al-Qarah Al-Hamra site (Sample 11) at 403.57 Bq $kg^{-1}$. Other notable concentrations were recorded at Qarah Sidi Musa (Sample 10; 304.51 Bq $kg^{-1}$), Al-Makhili (Sample 18; 257.94 Bq $kg^{-1}$), and Al-Kasarat (Sample 3; 249.77 Bq $kg^{-1}$). Conversely, the minimum concentration was found at the Tanmalu site (Sample 13), which measured 63.65 Bq $kg^{-1}$. A comparative analysis revealed that the mean activity concentrations of $^{40}K$, $^{238}U$, and $^{232}Th$ for the study area surpassed the corresponding worldwide average values of 400, 35, and 30 Bq $kg^{-1}$, respectively. Furthermore, the observed levels were elevated when compared to concentrations documented in many other geographical regions. While $^{40}K$ was a measurable component, its contribution to the total activity was marginal compared to the uranium and thorium series in these samples. The observed spatial heterogeneity in radionuclide distribution can be attributed to several factors, including the presence and nature of soil organic matter, the relative mobility of the radionuclides, seasonal fluctuations in the water table (which govern redox conditions), and vegetation cover that facilitates radionuclide retention. Globally, primordial radionuclides, including $^{40}K$, are the predominant source of natural ionizing radiation, accounting for approximately 83% of the annual effective dose to the world's population, with $^{40}K$ alone contributing about 16% [93].

***Table 2: Activity concentrations of radioactive potassium ($^{40}K$) in the studied samples***

| Simple No | Site Name | Radioactive potassium ($^{40}K$) |
|---|---|---|
| P1 | Aslanta | 145.57 |
| P2 | Wadi Atir | 79.01 |
| P3 | Sira Rajima | 248.21 |
| P4 | Jirdas | 98.63 |
| P5 | Freikh Mas'ada | 182.23 |
| P6 | Mas'ada | 180.38 |
| P7 | Al-Kasarat | 249.77 |
| P8 | Al-Halaqiema | 150.66 |
| P9 | Al-Qulay'at | 168.76 |
| P10 | Qara Sidi Musa | 304.51 |
| P11 | Al-Qara Al-Hamra | 403.57 |
| P12 | Zahr Al-Muhamadi | 206.35 |
| P13 | Tanmilu | 63.65 |
| P14 | Wadi Bousa'ida | 247.12 |
| P15 | Al-Thuban | 102.81 |
| P16 | Wadi Al-Qurna | 137.76 |
| P17 | Wadi Bil'atar | 208.29 |
| P18 | Al-Mukhayli | 257.94 |
| P19 | 2 North of the Gate District | 209.09 |
| P20 | 1 North of the Gate District | 108.32 |

***Radioactive Thorium ($^{232}Th$)***

Results presented in (Table 3) showed the activity concentrations of $^{232}Th$ in samples (1–20). The highest concentration was recorded in Sample 6 (Mas'ada site) at 63.18 Bq $kg^{-1}$, followed by: Sample 2 (Wadi A'tir site): 61.38 Bq $kg^{-1}$ Sample 15 (Al-Tha'ban site): 56.24 Bq $kg^{-1}$, Sample 1 (Aslunta site): 53.90 Bq $kg^{-1}$, Sample 3 (Siret Rajima site): 52.98 Bq $kg^{-1}$, Sample 10 (Qarah Sidi Musa site): 52.98 Bq $kg^{-1}$ Sample 14 (Wadi Busa'ida site): 51.69 Bq $kg^{-1}$Sample 14 (Farekh Mas'ada site): 50.88 Bq $kg^{-}$. Conversely, Sample 20 (1 North Al-Bawaba site) exhibited the lowest concentration at 31.16 Bq $kg^{-1}$ relative to other regional samples. The observed radioactivity in the collected soil samples may originate from radioactive heavy minerals enriched in $^{232}Th$ and $^{226}Ra$. This correlation suggests that thorium and uranium deposition occurred during the same geological period in the study area. The relatively high analyzed concentrations of $^{232}Th$ in certain soil samples indicate that thorium also contributed to environmental contamination. Thorium isotopes ($^{232}Th$) tend to be less mobile than uranium isotopes. Although the activity concentration of $^{232}Th$ is relatively high, its contribution remains minor compared to that of $^{226}Ra$. In practice, $^{232}Th$ is considered equivalent to $^{228}Th$ (and vice versa). The mean activity levels of $^{238}U$, $^{232}Th$, and $^{40}K$ in the granitoid samples were significantly lower than the global permissible averages of 32 Bq $kg^{-1}$, 45 Bq $kg^{-1}$, and 412 Bq $kg^{-1}$, respectively [91].


**Received**: 02-08-2025 - **Accepted**: 03-10-2025 - **Published**: 11-10-2025

Libyan Med J. 2025;17(3):366-377
https://doi.org/10.69667/lmj.2517402
Libyan Medical Journal
https://lmj.ly/index.php/ojs/index eISSN: 2079-1224

***Table 3: Activity concentrations of Radioactive Thorium ($^{232}Th$) in the studied samples***

| Simple No | Site Name | Radioactive Thorium ($^{232}Th$) |
|---|---|---|
| P1 | Aslanta | 53.90 |
| P2 | Wadi Atir | 61.38 |
| P3 | Sira Rajima | 52.98 |
| P4 | Jirdas | 41.44 |
| P5 | Freikh Mas'ada | 50.88 |
| P6 | Mas'ada | 63.18 |
| P7 | Al-Kasarat | 47.87 |
| P8 | Al-Halaqiema | 49.67 |
| P9 | Al-Qulay'at | 38.95 |
| P10 | Qara Sidi Musa | 52.75 |
| P11 | Al-Qara Al-Hamra | 41.66 |
| P12 | Zahr Al-Muhamadi | 42.19 |
| P13 | Tanmilu | 49.29 |
| P14 | Wadi Bousa'ida | 51.69 |
| P15 | Al-Thuban | 56.24 |
| P16 | Wadi Al-Qurna | 45.25 |
| P17 | Wadi Bil'atar | 45.77 |
| P18 | Al-Mukhayli | 37.34 |
| P19 | 2 North of the Gate District | 43.27 |
| P20 | 1 North of the Gate District | 31.16 |

***Radioactive Uranium ($^{238}U$)***

The activity concentrations of $^{238}U$ for the collected samples are detailed in Table 4. The maximum concentration was observed at the Wadi A'tir site (Sample 2), measuring 82.67 Bq $kg^{-1}$. Other notably high concentrations were recorded at Qarah Sidi Musa (Sample 10; 59.70 Bq $kg^{-1}$), Aslunta (Sample 1; 57.69 Bq $kg^{-1}$), and Wadi Busa'ida (Sample 14; 55.07 Bq $kg^{-1}$). In contrast, the minimum concentration was 32.48 Bq $kg^{-1}$, found at the 1 North Al-Bawaba site (Sample 20).

For comparative purposes, El Hassanin et al. (2006) reported uranium concentrations in analogous soils from the Qattara Depression region of Egypt to be between 5.1 and 6.9 mg $kg^{-1}$ (approximately 63–85 Bq $kg^{-1}$), which is broadly consistent with the findings of the current study. The observed variability in radionuclide concentrations is characteristic of regions impacted by extractive industries. While natural soils typically exhibit a constrained range of $^{226}Ra$ activity, those affected by mining often display a much wider and elevated range of concentrations. Consequently, the heightened $^{226}Ra$ levels detected in the study area may be indicative of the influence of historical or ongoing uranium mining activities.

Geochemically, uranium (U) exhibits significantly greater mobility in soil matrices compared to thorium (Th), rendering it more bioavailable. Despite their frequent co-occurrence in primary minerals, their biogeochemical behaviors diverge substantially. Uranium readily forms soluble complexes that enhance its uptake by flora, whereas thorium remains relatively immobile.

***Table 4: Activity concentrations of Radioactive Uranium ( $^{238}U$) in the studied samples***

| Simple No | Site Name | Radioactive Uranium ($^{238}U$) |
|---|---|---|
| P1 | Aslanta | 57.69 |
| P2 | Wadi Atir | 82.67 |
| P3 | Sira Rajima | 47.12 |
| P4 | Jirdas | 40.14 |
| P5 | Freikh Mas'ada | 52.71 |
| P6 | Mas'ada | 52.18 |
| P7 | Al-Kasarat | 48.35 |
| P8 | Al-Halaqiema | 45.39 |
| P9 | Al-Qulay'at | 38.35 |
| P10 | Qara Sidi Musa | 59.70 |
| P11 | Al-Qara Al-Hamra | 39.31 |
| P12 | Zahr Al-Muhamadi | 39.45 |


**Received**: 02-08-2025 - **Accepted**: 03-10-2025 - **Published**: 11-10-2025

Libyan Med J. 2025;17(3):366-377
https://doi.org/10.69667/lmj.2517402
Libyan Medical Journal
https://lmj.ly/index.php/ojs/index eISSN: 2079-1224

| | | |
|---|---|---|
| P13 | Tanmilu | 50.47 |
| P14 | Wadi Bousa'ida | 55.07 |
| P15 | Al-Thuban | 53.70 |
| P16 | Wadi Al-Qurna | 47.04 |
| P17 | Wadi Bil'atar | 41.36 |
| P18 | Al-Mukhayli | 41.03 |
| P19 | 2 North of the Gate District | 37.58 |
| P20 | 1 North of the Gate District | 32.48 |

***Radioactive Radium ($^{226}$Ra)***

As detailed in Table 5, the activity concentrations of $^{226}$Ra exhibited significant spatial variation across the sampling sites. The maximum concentration was observed at the Wadi A'tir site (Sample 2), measuring 96.48 Bq kg$^{-1}$. Other elevated concentrations were recorded at Tanmalu (Sample 13; 73.93 Bq kg$^{-1}$), Qarah Sidi Musa (Sample 10; 63.50 Bq kg$^{-1}$), and Wadi Busa'ida (Sample 14; 55.69 Bq kg$^{-1}$). In contrast, the minimum concentration was 34.00 Bq kg$^{-1}$ at the 1 North Al-Bawaba site (Sample 20).

The observed variability in radionuclide concentrations is largely a function of the soil's granulometric composition. It is well-established that radioactivity in soil is positively correlated with the proportion of fine-grained particles (e.g., clay) and inversely correlated with coarse-grained sand content. This phenomenon is attributed to the preferential adsorption and retention of radium atoms onto the larger specific surface area of fine grains. This principle, which has been corroborated by previous research [91-93], indicates that radionuclides are more readily concentrated within the structures and at the boundaries of fine-grained sediments compared to coarse-grained ones. Consequently, the relative proportions of clay and sand are key determinants of the activity concentrations for $^{226}$Ra, as well as for other primordial radionuclides like $^{238}$U and $^{232}$Th.

***Table 5: Activity concentrations of Radioactive Thorium (226 Th) in samples (1–20)***

| Simple No | Site Name | Radioactive Radium ($^{226}$Ra) |
|---|---|---|
| P1 | Aslanta | 51.08 |
| P2 | Wadi Atir | 96.48 |
| P3 | Sira Rajima | 43.93 |
| P4 | Jirdas | 38.42 |
| P5 | Freikh Mas'ada | 46.27 |
| P6 | Mas'ada | 45.77 |
| P7 | Al-Kasarat | 48.51 |
| P8 | Al-Halaqiema | 52.77 |
| P9 | Al-Qulay'at | 32.01 |
| P10 | Qara Sidi Musa | 63.50 |
| P11 | Al-Qara Al-Hamra | 38.93 |
| P12 | Zahr Al-Muhamadi | 38.00 |
| P13 | Tanmilu | 73.93 |
| P14 | Wadi Bousa'ida | 55.69 |
| P15 | Al-Thuban | 48.33 |
| P16 | Wadi Al-Qurna | 42.49 |
| P17 | Wadi Bil'atar | 38.85 |
| P18 | Al-Mukhayli | 36.48 |
| P19 | 2 North of the Gate District | 38.78 |
| P20 | 1 North of the Gate District | 34.00 |

## Discussion

The observed elevated concentrations of $^{40}$K, $^{238}$U, and $^{232}$Th suggest contributions from both anthropogenic and gelogenic sources. The heightened levels of $^{40}$K may be attributed to the application of potassium-rich inorganic fertilizers in adjacent agricultural practices. Similarly, elevated $^{238}$U concentrations can be linked to the continuous use of phosphate fertilizers, which are employed to amend nutrient-depleted soils resulting from intensive agriculture and erosion. Phosphate rock, the primary raw material for these fertilizers, is inherently enriched in uranium. From a geological perspective, the local lithology likely plays a significant role. The presence of radionuclide-enriched lithologies, such as carbonatite and monazite,


**Received**: 02-08-2025 - **Accepted**: 03-10-2025 - **Published**: 11-10-2025

Libyan Med J. 2025;17(3):366-377
https://doi.org/10.69667/lmj.2517402
Libyan Medical Journal
https://lmj.ly/index.php/ojs/index eISSN: 2079-1224

can account for the elevated $^{238}U$ values. While granitic rocks are globally recognized for their high uranium and thorium content, the mean activity concentrations measured in the granitoid samples from this study were lower than established global averages of 412 Bq $kg^{-1}$ for $^{40}K$, 32 Bq $kg^{-1}$ for $^{238}U$, and 45 Bq $kg^{-1}$ for $^{232}Th$, respectively [91].

During magmatic crystallization, uranium and thorium are incorporated into the rock matrix, potentially influencing the composition of surrounding geological formations, including the metasedimentary and metavolcanic units (e.g., fluorites, quartzites, schists) prevalent in the study area. The environmental transport and subsequent health risks associated with these radionuclides are governed by their distinct physicochemical properties. Uranium, being relatively soluble, can migrate in aqueous solutions and bind to clay minerals, whereas thorium exhibits low solubility and remains largely immobile. Prolonged human exposure to the decay chains of uranium and thorium, primarily through inhalation, is associated with severe health outcomes, including chronic pulmonary diseases, hematological disorders such as leukopenia and anemia, and tissue necrosis. A standard methodological approach in such investigations involves estimating the activity of a parent isotope from its progeny under the assumption of secular equilibrium. The validity of this assumption in the current study was confirmed, as the calculated activity ratios within the uranium, actinium, and thorium series were found to approximate unity [95].

The geochemical partitioning of radionuclides significantly influences their observed distribution. The relative resistance of thorium-bearing minerals to weathering processes can lead to their enrichment and accumulation in specific soil samples. Conversely, uranium's higher susceptibility to leaching and mobilization can result in its transport and subsequent concentration in secondary locations. Nevertheless, the elevated radionuclide concentrations observed are predominantly attributed to the natural enrichment of the local granitic bedrock, which contains substantial amounts of uranium, thorium, and potassium minerals. Statistical analysis of the activity concentration data revealed distinct distribution patterns. The $^{232}Th$ data exhibited a positive skew, indicating an asymmetric distribution with a tail towards higher concentrations. In contrast, the $^{238}U$ and $^{40}K$ datasets showed negative skewness, suggesting a bias towards lower values (Heckman et al., 2002). Crucially, the measured activity concentrations of $^{40}K$, $^{232}Th$, and $^{226}Ra$ in all soil samples were below the corresponding global averages. Furthermore, all calculated radiological hazard parameters—including absorbed dose rates, annual effective doses, radium equivalent activity (Raeq), and external/internal hazard indices—were also lower than the recommended limits reported by UNSCEAR (2000). While the primary source is geological, variability in soil radioactivity can also be influenced by anthropogenic activities, such as the storage and application of phosphate-based fertilizers, which are known to contain elevated levels of U-238, Th-232, and Ra-226. Gamma radiation from naturally occurring radionuclides—specifically $^{40}K$ and the decay progeny of the $^{238}U$ and $^{232}Th$ series—constitutes the primary component of terrestrial background radiation to which humans are externally exposed [96]. The magnitude of this terrestrial radiation is fundamentally controlled by local lithology. For instance, igneous rocks of granitic composition are typically enriched in thorium and uranium, whereas basaltic and ultrabasic rocks exhibit very low concentrations. Sedimentary rocks generally have lower radionuclide content, with notable exceptions such as phosphate and clay-rich formations [97].

A strong positive correlation was observed between the ambient equivalent dose rates measured in situ by survey meters and the dose rates estimated from the in-situ activity concentrations of K-40, Ra-226, and Th-232 in the collected rock and soil samples. However, the estimated values were consistently lower than the directly measured values. This discrepancy is a well-documented phenomenon, with global data indicating that air-absorbed dose rates derived from soil samples can differ from direct measurements by up to 50%, a variance attributable to multiple factors that influence field-based measurements.

When benchmarked against the global averages reported by the United Nations Scientific Committee on the Effects of Atomic Radiation (UNSCEAR)—33 Bq $kg^{-1}$ for $^{238}U$, 45 Bq $kg^{-1}$ for $^{232}Th$, 32 Bq $kg^{-1}$ for $^{226}Ra$, and 420 Bq $kg^{-1}$ for $^{40}K$—the mean activity concentrations measured in this study were found to be substantially lower. This contrasts with findings from mining-impacted regions, such as a study of eastern Ugandan quarries, which reported significantly elevated activity concentrations and outdoor annual effective dose rates (0.30–1.37 mSv $y^{-1}$) that far exceed the global average of 0.07 mSv $y^{-1}$ [91]. Such elevated levels underscore the potential for anthropogenic activities, particularly mining, to enhance background radiation and pose a radiological hazard.

The distribution of these primordial radionuclides is fundamentally controlled by local geology and mineralogy. For instance, thorium and uranium are commonly concentrated in accessory minerals like monazite, which forms from the weathering of granitic rocks, while $^{40}K$ is predominantly associated with K-feldspars and micas. The enrichment of uranium and thorium in granitic plutons is a consequence of their geochemical behavior; their large ionic radii inhibit incorporation into early-forming silicate minerals, leading to their concentration in late-stage magmatic fluids and crystallization products. These processes,


**Received**: 02-08-2025 - **Accepted**: 03-10-2025 - **Published**: 11-10-2025

**Libyan Med J.** 2025;17(3):366-377
https://doi.org/10.69667/lmj.2517402
**Libyan Medical Journal**
https://lmj.ly/index.php/ojs/index *eISSN: 2079-1224*

along with the potential accumulation of radionuclide-rich tailings, can explain localized variations in activity concentrations.

To collectively assess the radiological risk from the measured $^{238}U$, $^{232}Th$, and $^{40}K$ concentrations, the Radium Equivalent Activity (R_eq) index is utilized. This hazard index provides a single comparative value for the gamma radiation exposure from a mixture of radionuclides. The R_eq is calculated based on the premise that 370 Bq $kg^{-1}$ of $^{226}Ra$, 259 Bq $kg^{-1}$ of $^{232}Th$, and 4,810 Bq $kg^{-1}$ of $^{40}K$ yield an identical gamma dose rate. Materials with an R_eq value exceeding 370 Bq $kg^{-1}$ are considered to pose an unacceptable radiation hazard. This threshold corresponds to an annual effective dose of 1 mSv for the general public, which is the recommended dose limit [98].

## Conclusion

This study successfully quantified the concentrations of the primordial radionuclides $^{40}K$, $^{238}U$, $^{232}Th$, and $^{226}Ra$ within the investigated sites. A comprehensive assessment of the associated radiation hazard indices confirmed that all values were well below internationally recommended safety limits. Although the measured radionuclide concentrations exhibited spatial variability across the study area, they remained within permissible thresholds. Consequently, the study area is confirmed to contain significant quantities of these natural radioactive elements that, according to global standards, pose no significant radiological hazard and hold potential for beneficial utilization.

***Acknowledgment***

The authors highly appreciated the help of the physical radiation of the Physics Department, Omar Al-Muktar University, during the radioactive elements analysis of this study.

***Conflict***

No conflict of the results recorded in this study with other studies.

## References

1. Olagbaju PO, Wojuola OB, Tshivhase V. Radionuclides contamination in soil: effects, sources and spatial distribution. EPJ Web Conf. 2021;253:01005.
2. Yadav M, Jindal MK, Ramola R. Study of radionuclides in rocks samples from Ukhimath area and its correlation with soil and water data. Chem Afr. 2023;6:2165–73.
3. Onjefu SA, Kauluma AN, Zivuku M, Ejembi E, Hamunyela RH, Tyobek BM, et al. Assessment of radioactivity levels in shore sediments along the coastline of the Orange River, Oranjemund, Namibia. Heliyon. 2022;8:e10579.
4. Rabiu JA, Raheem IO, Kolawole AA, Adeniji QA, Aruna N. Health implications of radiation hazards from soil in residential areas of Maiganga mining site in Gombe State of Nigeria. Niger J Phys. 2021;30(2):1-17.
5. Orosun MM, Ajibola TB, Akinyose FC, Osanyinlusi O, Afolayan OD, Mahmud MO. Assessment of ambient gamma radiation dose and annual effective dose associated with radon in drinking water from gold and lead mining area of Moro, North-Central Nigeria. J Radioanal Nucl Chem. 2021;328:129–36.
6. Hamad R, Ikraiam F, Hasan H. Determination of specific natural radionuclides in the bones of some local fish commonly consumed from the eastern Libyan coast. J Rad Nucl Appl. 2023;8(3):283-9.
7. Sroor AT, Walley El-Dine N, El-Bahi SM, Hasa HMA, Ali JM. Determination of radionuclides levels and absorbed dose for soil, rock, plant and water in gondola- Libya. IOSR J Appl Phys. 2018;10(4):40-9.
8. Hasan H, Ammhmmid R, Khatab H, Ali J, Al kaseh A. Using gamma ray radiation to estimate the types and contents of radioactive nuclides in some ported sugar samples, Libya. AlQalam J Med Appl Sci. 2025;8(3):1795-803.
9. Hamad IH, Nuesry MS. The poly cyclic hydrocarbons levels in some fishes tissues collected from Derna City (Libya) Coast. In: International conference on chemical, agricultural and medical sciences; 2014 Dec 4-5; Antalya, Turkey. 2014. p. 52-6.
10. Hamad MAH, Mounera AAE, Baseet ESM, Eman E, Al-Badri M. Identification and detection the aromatic and aliphatic hydrocarbons in Epinephelus Marginatus fish samples collected from Benghazi coast. Int J Adv Multidiscip Res Stud. 2023;6(3):107-13.
11. Mohammed A, Hamad MAH, Mounera AAE, Eman IHE. Extraction and identification of aliphatic hydrocarbons in marine sediment samples at Benghazi city and Dyriana town coasts (Libya). J Res Humanit Soc Sci. 2023;11(10):168-74.
12. Hasan MAH, Muftah HS, Abdelghani KA, Saad SI. Poly aromatic hydrocarbon concentrations in some shell samples at some Tobrouk city coast regions: could the oil industry be significantly affecting the environment. Ukr J Ecol. 2022;12(3):21-8.
13. Habel AMA, Mohamed NIH, Mohammed MA, Hamad MAH. The levels and sources of aliphatic and polycyclic aromatic hydrocarbons in blue runner fish from Benghazi coast, Libya. Afr J Biol Sci. 2024;6(3):1-10.
14. Hasan HMI, Mohamad ASA. A study of aliphatic hydrocarbons levels of some waters and sediments at Al-Gabal Al-Akhder coast regions. Int J Chem Sci. 2013;11(2):833-49.


***Received****: 02-08-2025 -* ***Accepted****: 03-10-2025 -* ***Published****: 11-10-2025*

**Libyan Med J.** 2025;17(3):366-377
https://doi.org/10.69667/lmj.2517402
**Libyan Medical Journal**
*https://lmj.ly/index.php/ojs/index eISSN: 2079-1224*

15. Salem GM, Aljidaemi FF, Hwisa SA, Hamad MIH, Zaid AA, Amer IO, et al. Occupational exposure to benzene and changes in hematological parameters in East Tripoli, Libya. Nanotechnol Percept. 2024;20(S5):358-64.
16. Habil Z, Ben arous N, Masoud N, Hasan H. Using GC-mass method for determination the hydrocarbon compounds in some vegetable samples at Derna city, Libya. Libyan Med J. 2025;17(3):374-83.
17. Hasan H, Habil Z, Ben arous N. Estimate the types and contents of phenolic acid in C.Paviflorus lam and C.salviiflolius L plants growing at Al –Gabal Al-hder regions. AlQalam J Med Appl Sci. 2025;8(3):1646-56.
18. Alfutisi H, Hasan H. Removing of thymol blue from aqueous solutions by pomegranate peel. EPH Int J Appl Sci. 2019;1(1):111-9.
19. Hasan JA, Hasan HMA. Potential human health risks assessment through determination of heavy metals contents in regularly consumed yogurta in Libya. World J Pharm Pharm Sci. 2024;13(12):100-12.
20. Mamdouh SM, Wagdi ME, Ahmed MA, Alaa EA, Essam AM, Hamad MIH. Rice husk and activated carbon for waste water treatment of El-Mex Bay, Alexandria Coast, Egypt. Arab J Chem. 2016;9(S2):S1590-S6.
21. Mamdouh SM, Wagdi ME, Ahmed MA, Alaa EA, Hamad IH. Heavy metals accumulation in sediments of Alexandria coastal areas. Bull Fac Sci. 2012;47(1-2):12-28.
22. Mamdouh SM, Wagdi ME, Ahmed MA, Hamad MIH. Chemical studies on Alexandria coast sediment. Egypt Sci Mag. 2005;2(4):93-102.
23. Mamdouh SM, Wagdi ME, Ahmed MA, Alaa EA, Hamad MIH. Distribution of different metals in coastal waters of Alexandria, Egypt. Egypt Sci Mag. 2010;7(1):1-19.
24. Mohamed AE, Afnan SA, Hamad MA, Mohammed AA, Mamdouh SM, Alaa RE, et al. Usage of natural wastes from animal and plant origins as adsorbents for the removal of some toxic industrial dyes and heavy metals in aqueous media. J Water Process Eng. 2023;55:104192.
25. Mohamed HB, Mohammed AZ, Ahmed MD, Hamad MAH, Doaa AE. Soil heavy metal pollution and the associated toxicity risk assessment in Ajdabiya and Zueitina, Libya. Sci J Damietta Fac Sci. 2024;14(1):16-27.
26. Nabil B, Hamad H, Ahmed E. Determination of Cu, Co and Pb in selected frozen fish tissues collected from Benghazi markets in Libya. Chem Methodol. 2018;2:56-63.
27. Wesam FAM, Hamad MAH. Detection of heavy metals and radioactivity in some bones of frozen chicken samples collected from Libyan markets. Int J Adv Multidiscip Res Stud. 2023;3(3):761-4.
28. Wesam FAM, Hamad MAH. Study the accumulation of minerals and heavy metals in Ulva algae, Cladophora, Polysiphonia and Laurencia algae samples at eastern north region of Libya coast. GSC Biol Pharm Sci. 2023;23(03):147-52.
29. Citrine E, Hamad H, Hajer Af. Contents of metal oxides in marine sediment and rock samples from the eastern Libyan coast, utilizing the X-ray method. AlQalam J Med Appl Sci. 2015;1(1):1316-21.
30. Hanan MA, Hamida E, Hamad MAH. Nitrogen, phosphorus and minerals (Sodium, Potassium and Calcium) contents of some algae's species (Anabaena and Spirulina platensis). Int J Curr Microbiol App Sci. 2016;5(11):836-41.
31. Mardhiyah F, Hamad H. Assessment of soil contamination by heavy metals in the Al-Fatayeh Region, Derna, Libya. AlQalam J Med Appl Sci. 2025;8(3):1081-91.
32. Abdelrazeg A, Khalifa A, Mohammed H, Miftah H, Hamad H. Using melon and watermelon peels for the removal of some heavy metals from aqueous solutions. AlQalam J Med Appl Sci. 2025;8(3):787-96.
33. Abdul Razaq A, Hamad H. Estimate the contents and types of water well salts by the Palmer Roger model affecting the corrosion of Al-Bayda city (Libya) network pipes. AlQalam J Med Appl Sci. 2025;8(3):744-53.
34. Abdulsayid FA, Hamad MAH, Huda AE. IR spectroscopic investigation, X-ray fluorescence scanning, and flame photometer analysis for sediments and rock samples of Al-Gabal Al-Akhder coast region (Libya). IOSR J Appl Chem. 2021;14(4):20-30.
35. ALambarki M, Hasan HMA. Assessment of the heavy metal contents in air samples collected from the area extended between Albayda and Alquba cities (Libya). AlQalam J Med Appl Sci. 2025;8(3):695-707.
36. Al-Nayyan N, Mohammed B, Hamad H. Estimate of the concentrations of heavy metals in soil and some plant samples collected from (near and far away) of the main road between Al-Bayda city and Wadi Al-Kouf region. AlQalam J Med Appl Sci. 2025;8(3):816-26.
37. Hasan HMI. Studies on physicochemical parameters and water treatment for some localities along coast of Alexandria [Doctoral dissertation]. Alexandria University; 2006.
38. Hamad MAH, Hager AA, Mohammed EY. Chemical studies of water samples collected from area extended between Ras Al–Halal and El Haniea, Libya. Asian J Appl Chem Res. 2022;12(3):33-46.
39. Hamad M, Mohammed AA, Hamad MAH. Adsorption and kinetic study for removal some heavy metals by use in activated carbon of sea grasses. Int J Adv Multidiscip Res Stud. 2024;4(6):677-85.
40. Hamad MAH, Hamad NI, Mohammed MYA, Hajir OAA, Al-Hen dawi RA. Using bottom marine sediments as environmental indicator state of (Tolmaitha – Toukra) region at eastern north coast of Libya. Sch J Eng Tech. 2024;2(14):118-32.
41. Hamad MIH. The heavy metals distribution at coastal water of Derna city (Libya). Egypt J Aquat Res. 2008;34(4):35-52.
42. Hamad MIH, Islam MU. The concentrations of some heavy metals of Al-Gabal Al-Akhdar Coast Sediment. Arch Appl Sci Res. 2010;2(6):59-67.
43. Hamad MAH, Amira AKA. Estimate the concentrations of some heavy metals in some shoes polish samples. EPH Int J Appl Sci. 2016;2(2):24-7.


***Received****: 02-08-2025 -* ***Accepted****: 03-10-2025 -* ***Published****: 11-10-2025*

**Libyan Med J.** 2025;17(3):366-377
https://doi.org/10.69667/lmj.2517402
**Libyan Medical Journal**
*https://lmj.ly/index.php/ojs/index eISSN: 2079-1224*

44. Hamad MAH, Hussien SSM, Basit EEM. Accumulation of some heavy metals in green algae as bio indicators of environmental pollution at Al-Haniea region: Libya coastline. Int J Adv Multidiscip Res Stud. 2024;4(5):188-90.
45. Hamad MIH, Ahmed MA. Major cations levels studies in surface coastal waters of Derna city, Libya. Egypt J Aquat Res. 2009;35(1):13-20.
46. Hamad MIH, Masoud MS. Thermal analysis (TGA), diffraction thermal analysis (DTA), infrared and X-rays analysis for sediment samples of Toubrouk city (Libya) coast. Int J Chem Sci. 2014;12(1):11-22.
47. Hamad R, Ikraiam FA, Hasan H. Estimation of heavy metals in the bones of selected commercial fish from the eastern Libyan coast. J Rad Nucl Appl. 2024;9(1):47-51.
48. Hasan HAH. Estimate lead and cadmium contents of some archeological samples collected from ancient cities location (Cyrene and Abolonia) at Al-Gabal Al-Akhder Region, Libya. Univ J Chem Appl. 2021;12(21):902-7.
49. Eltawaty SA, Abdalkader GA, Hasan HM, Houssein MA. Antibacterial activity and GC-MS analysis of chloroform extract of bark of the Libyan Salvia fruticosa Mill. Int J Multidiscip Sci Adv Technol. 2021;1(1):715-21.
50. Aljamal MA, Hasan HM, Al Sonosy HA. Antibacterial activity investigation and anti-biotic sensitive's for different solvents (Ethanol, propanol, DMSO and di Ethel ether) extracts of seeds, leafs and stems of (Laurus azorica and Avena sterilis) plants. Int J Curr Microbiol App Sci. 2024;13(11):175-90.
51. Hamade MH, Abdelraziq SA, Gebreel AA. Extraction and determination the of Beta carotene content in carrots and tomato samples collected from some markets at ElBeida City, Libya. EPH Int J Appl Sci. 2019;1(1):105-10.
52. Hasan HM, Ibrahim H, Gonaid MA, Mojahidul I. Comparative phytochemical and antimicrobial investigation of some plants growing in Al Jabal Al-Akhdar. J Nat Prod Plant Resour. 2011;1(1):15-23.
53. Hasan H, Jadallah S, Zuhir A, Ali F, Saber M. The Anti-Cancer, Anti-Inflammatory, Antibacterial, Antifungal, Anti-Oxidant and phytochemical investigation of flowers and stems of Anacyclus Clavatus plant extracts. AlQalam J Med Appl Sci. 2025;8(3):415-27.
54. Hasan H, Zuhir A, Shuib F, Abdraba D. Phytochemical investigation and exploring the Citrullus Colocynthis extracts as antibacterial agents against some gram and negative bacteria species. AlQalam J Med Appl Sci. 2025;8(3):392-400.
55. MdZeyaullah R, Naseem A, Badrul I, Hamad MI, Azza SA, Faheem AB, et al. Catechol biodegradation by Pseudomonas strain: a critical analysis. Int J Chem Sci. 2009;7(3):2211-21.
56. El-Mehdawy MF, Eman KS, Hamad MI, Hasan H. Amino acids contents of leafs and stems for two types of herbal plants (Marjoram and Hybrid tea rose) at AL-Gabal AL-Akhder region. Der Pharma Chem. 2014;6(6):442-7.
57. El-Mehdawy MF, Eman KS, Hamad MIH. Amino acid contents of leafs and stems for three types of herbal plants at Al-Gabal Al-Akhder region. World J Chem. 2014;9(1):15-9.
58. Hamad MH, Noura AAM, Salem AM. Phytochemical screening, total phenolic, anti-oxidant, metal and mineral contents in some parts of plantago Albicans grown in Libya. World J Pharm Res. 2024;13(3):1-17.
59. Anees AS, Hamad MIH, Hasan H, Mojahidul I. Antifungal potential of 1,2-4triazole derivatives and therapeutic efficacy of Tinea corporis in albino rats. Der Pharm Lett. 2011;3(1):228-36.
60. Hamad H, Marwa M, Amal H. Determining the contents of antioxidants, total phenols, carbohydrate, total protein, and some elements in Eucalyptus gomphocephala and Ricinus communis plant samples. Libyan Med J. 2015;1(1):222-31.
61. Hamad H, Zuhir A, Farag S, Dala A. Efficiency of Cynara Cornigera fruits on antibacterial, antifungal and its phytochemical, anti-oxidant screening. Libyan Med J. 2025;3(1):120-8.
62. Hamad H, Ashour S, Ahmed A. Estimation of amino acid composition, total carbohydrate, and total protein content in Ballota pseudodictamnus plant extracts from Al Jabal Al Akhdar Region, Libya. Libyan Med J. 2025;3(1):266-71.
63. Hamad H, Ahmed H, Wafa A. Evaluation of anti-oxidant capacity, total phenol, metal, and mineral contents of Ziziphus lotus plant grown at some regions of AlGabal AlKhder, Libya. Libyan Med J. 2025;3(1):137-43.
64. Ben Arous NA, Naser ME, Hamad MAH. Phytochemical screening, anti-bacterial and anti-fungi activities of leafs, stems and roots of C. parviflorus Lam and C. salviifolius L plants. Int J Curr Microbiol App Sci. 2014;13(11):262-80.
65. Anas FAE, Hamad MAH, Salim AM, Azza MH. Phytochemical screening, total phenolics, antioxidant activity and minerals composition of Helichrysum stoechas grown in Libya. Afr J Biol Sci. 2024;3(6):2349-60.
66. Naseer RE, Najat MAB, Salma AA, Hamad MAH. Evaluation of metal and mineral contents of leafs, stems and roots of C. Parviflorus Lam and C. Salviifolius L plants growing at Al Ghabal Al-Khder (Libya). Int J Adv Multidiscip Res Stud. 2024;4(5):191-4.
67. Hamad MAH, Salem AM. Total carbohydrate, total protein, minerals and amino acid contents in fruits, pulps and seeds of some cultivars of muskmelon and watermelon fruit samples collected from Algabal Alkhder region. Sch J Appl Med Sci. 2024;12(1):1-7.
68. Gonaid MI, Ibrahim H, Al-Arefy HM. Comparative chemical and biological studies of Salvia fruticosa, Ocimum basillicum and Pelergonium graveolans cultivated in Al-Jabal Al- AkhdarAkhdar. J Nat Prod Plant Resour. 2012;6(2):705-10.
69. Rinya FMA, Hamad MAH, Ahlam KA, Hammida MEH. Phytochemical screening of some herbal plants (Menthe, Origanum and Salvia) growing at Al-Gabal Al-akhder Region-Libya. Afr J Basic Appl Sci. 2017;9(3):161-4.


***Received***: *02-08-2025* - ***Accepted***: *03-10-2025* - ***Published***: *11-10-2025*

70. Anas FAA, Hamad MAH, Salim AA, Azza MH. Phytochemical screening, total phenolics, antioxidant activity and minerals composition of Helichrysum stoechas grown in Libya. Afr J Biol Sci. 2024;3(6):2349-60.
71. Haroon A, Hasan H, Wafa AAS, Baset ESM. A comparative study of morphological, physiological and chemical properties of leafs and steam samples of (E.gomphocephala) (Tuart) plant growing at coastal (Derna city) and …. J Res Environ Earth Sci. 2024;9(12):10-8.
72. Hamad MAS, Ali AR. Separation and identification the speciation of the phenolic compounds in fruits and leaves of some medicinal plants (Juniperus phoenicea and Quercus coccifera) growing at Algabal Al Akhder region, Libya. Indian J Pharm Educ Res. 2016;51(3):299-303.
73. Enam FM, Wesam FAM, Hamad MAH. Detection the contents of minerals of (Sodium, Potassium and Calcium) and some metals of (Iron, Nickel and Copper) in some vegetable and soil samples collected from Al-Marj. Int J Adv Multidiscip Res Stud. 2023;5(3):304-9.
74. Hamad MIH, Mousa SR. Synthesis and (IR and TEM) characterization of leafs and stem nanoparticles of Artemisia plant: comparative study for the evaluation of anti-bacterial efficiency. Int J Adv Multidiscip Res Stud. 2024;4(5):195-9.
75. Elsalhin H, Abobaker HA, Hasan H, El–Dayek GA. Antioxidant capacity and total phenolic compounds of some algae species (Anabaena and Spirulina platensis). Sch Acad J Biosci. 2016;4(10):782-6.
76. Alaila AK, El Salhin HE, Ali RF, Hasan HM. Phytochemical screening of some herbal plants (Menthe, Origanum and Salvia) growing at al-gabal al-akhder region- Libya. Int J Pharm Life Sci. 2017;8(4):5500-3.
77. Hasan H, Mariea FFE, Eman KS. The contents of some chemical compounds of leafs and stems of some herbal plants (Thymy, Rosemary, Salvia, Marjoram and Hybrid Tea Rose) at Al-Gabal Al-Akhder region. EPH Int J Appl Sci. 2014;6(3):1-8.
78. El-Mehdawe MF, Eman KS, Hamad MIH. Heavy metals and mineral elements contents of leafs and stems for some herbal plants at AL-Gabal AL-Akhder region. Chem Sci Rev Lett. 2014;3(12):980-6.
79. Hamad MIH, Aaza IY, Safaa SHN, Mabrouk MS. Biological study of transition metal complexes with adenine ligand. Proc. 2019;41(1):77.
80. Ahmed ONH, Hamad MAH, Fatin ME. Chemical and biological study of some transition metal complexes with guanine as ligand. Int J New Chem. 2023;10(3):172-83.
81. Hamad MAH, Enas UE, Hanan AK, Hana FS, Somia MAE. Synthesis, characterization and antibacterial applications of compounds produced by reaction between Barbital with Threonine, glycine, lycine, and alanine. Afr J Biol Sci. 2024;6(4):1-10.
82. Emrayed H, Hasan H, Liser R. Corrosion inhibition of carbon steel using (Arginine –levofloacin-metal) complexes in acidic media. AlQalam J Med Appl Sci. 2025;8(3):1633-40.
83. Hasan H, Abdelgader I, Emrayed H, Abdel-Gany K. Removal of the medical dye safranin from aqueous solutions by sea grasses activated carbon: a kinetic study. AlQalam J Med Appl Sci. 2025;8(3):428-34.
84. Hasan HMA, Alhamdy MA. Adsorption and kinetic study for removal some heavy metals by using activated carbon of sea grasses. Int J Adv Multidiscip Res Stud. 2024;4(6):677-85.
85. Almadani EA, Hamad MAH, Kwakab FS. Kinetic study of the adsorption of the removal of bromo cresol purple from aqueous solutions. Int J Res Granthaalayah. 2019;7(12):1-10.
86. Mamdouh SM, Wagdi ME, Ahmed MA, Alaa EA, Essam AM, Hamad MIH. Rice husk and activated carbon for waste water treatment of El-Mex Bay, Alexandria Coast, Egypt. Arab J Chem. 2016;9(S2):S1590-S6.
87. Hasan H, El-maleh C. Evaluation of some heavy metal levels in tissue of fish collected from coasts of susa region, libya. Attahadi Med J. 2025;1(1):118-22.
88. Balal A, Obid M, Khatab H, Hasan H. Determination of lead and cadmium marine water and crabs (pachygrapsus marmoratus) from tolmitha coast, Libya. AlQalam J Med Appl Sci. 2025;8(3):1670-7.
89. Abdull-Jalliel H, Sulayman A, Alhoreir M, Hasan H. The antimicrobial effect of some metal concentration on growth of staphylococcus and klebsiella bacteria species. AlQalam J Med Appl Sci. 2025;8(3):1646-56.
90. Abdull–Jalliel H, B Arous N, Alhoreir M, Hasan H. Using the extracts of the (Dodder) plant and the concentrations of some metals as inhibitors for growth, the (Pseudomonas) bacteria isolated from some hospital rooms in Derna and Al bayda. AlQalam J Med Appl Sci. 2025;8(3):1600-11.
91. Qureshi AA, Tariq S, Kamal U, Manzoor S, Calligaris C, Waheed A. Science Direct Evaluation of excessive lifetime cancer risk due to natural radioactivity in the rivers sediments of Northern Pakistan. J Radiat Res Appl Sci. 2014;7:438–47.
92. United Nations Scientific Committee on the Effects of Atomic Radiation. Sources and effects of ionizing radiation: Sources. New York: United Nations; 2000.
93. Ghorbanipour M, Alhashemi A, Gharloghi S, Adeli M, Gholami M. Health risk assessment of natural background radiation in residents of Khorramabad, Iran. Iran J Med Phys. 2019;14:23–8.
94. Faanu A, Darko EO, Ephr JH. Determination of natural radioactivity and hazard in soil and rock samples in a mining area in Ghana. West Afr J Appl Ecol. 2010;19:77-92.
95. Dhawal SJ, Kulkarni GS, Pawar SH. Terrestrial background radiation studies in south Konkan, Maharashtra, India. Int J Radiat Res. 2013;11(4):263–7.
96. El-Gamal AA, Saleh IH. Radiological and mineralogical investigation of accretion and erosion coastal sediments in Nile Delta Region, Egypt. J Oceanogr Mar Sci. 2012;3(3):41–55.
97. Zaim N, Tugrul A, Atlas H, Buyuk B, Demir E, Baydogan N, et al. Investigation of natural radioactivity of surface soil samples in the vicinity of Edirne, Turkey. Acta Phys Pol A. 2016;130(1):64–7.
98. El-Taher A. Elemental analysis of two Egyptian phosphate rock mines by instrumental neutron activation analysis and atomic absorption spectrometry. Appl Radiat Isot. 2016;68(3):511-5.


***Received****: 02-08-2025 -* ***Accepted****: 03-10-2025 -* ***Published****: 11-10-2025*